

Learning nonlinear hybrid automata from input–output time-series data

Amit Gurung[✉], Masaki Waga[✉], and Kohei Suenaga[✉]

Graduate School of Kyoto University, Kyoto, Japan
rajgurung777@gmail.com, {mwaga, ksuenaga}@fos.kuis.kyoto-u.ac.jp

Abstract. Learning an automaton that approximates the behavior of a black-box system is a long-studied problem. Besides its theoretical significance, its application to search-based testing and model understanding is recently recognized. We present an algorithm to learn a nonlinear hybrid automaton (HA) that approximates a black-box hybrid system (HS) from a set of input–output traces generated by the HS. Our method is novel in handling (1) both exogenous and endogenous HS and (2) HA with reset associated with each transition. To our knowledge, ours is the first method that achieves both features. We applied our algorithm to various benchmarks and confirmed its effectiveness.

Keywords: Automata Learning · Inferring Hybrid Systems · Learning Cyber-Physical Systems.

1 Introduction

Mathematical modeling of the behavior of a system is one of the main tasks in science and engineering. If a system exhibits only continuous dynamics, it is well modeled by ordinary differential equations (ODE). However, many systems exhibit continuous and discrete dynamics, being instances of *hybrid systems* (HS). For instance, in modeling an automotive engine, the ODE must be switched following the status of the gear. A similar combination of continuous and discrete dynamics also appears in many other systems, e.g., biological systems [5].

Hybrid automata (HAs) [3] is a formalism for HS. Fig. 1 illustrates an HA modeling a bouncing ball. In an HA, a set of locations (represented by a circle in Fig. 1) and transitions between them (represented by an arrow) expresses its discrete dynamics. An ODE as-

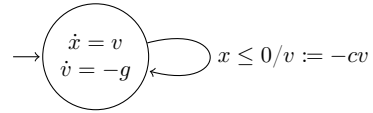


Fig. 1: A bouncing ball model

sociated with each location expresses continuous dynamics. In the HA in Fig. 1, the ODEs at the location show the free-fall behavior of the system, and the transition shows the discrete jump caused by bouncing on the floor (i.e., a change in the ball’s velocity.)

It is a natural research direction to automatically identify an HA given system’s behavior. Not only is it interesting as research, but it is also of a practical impact since learning a model of a black-box system is recently being applied to

Table 1: Comparison of hybrid automata learning methods

	Non-linear ODEs?	Exo- and Endogenous?	Infer Resets?	Support Inputs?
Ours	Polynomial	Yes	Yes	Yes
[16]	Polynomial	Only Exogenous	No	Yes
[26]	Linear	Yes	No	Yes*
[20, 21]	Linear	Only Endogenous	No	No

* Although this feature is claimed in the paper, the available implementation does not support it.

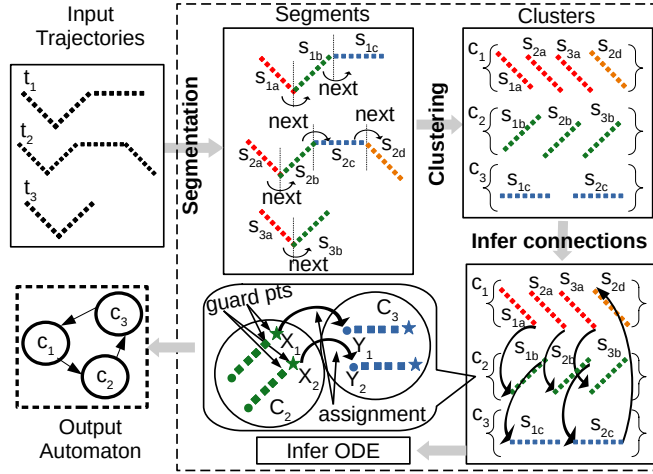


Fig. 2: Overview of our HA learning algorithm. In the below center figure, the circle and the star points stand for each segment's first and last points.

automated testing (e.g., black-box checking [15, 19, 24].) There have been various techniques to infer an HA from a set of input-output system trajectories. However, as Table 1 shows, all the existing methods have some limitations in the inferred HA. To the best of our knowledge, there is no existing work that achieves all of the following features: (1) Learned HAs may involve nonlinear ODE as a flow; (2) Learned HAs may be exogenous (i.e., mode changes caused by external events) and endogenous (i.e., mode changes caused by internal events); and (3) Learned HAs may involve resetting of variables at a transition.

This paper proposes an HA-learning algorithm that achieves the three features above. Namely, our algorithm learns an HA that may be exogenous, endogenous or both. A learned HA can reset variables at transitions. These two features make it possible to infer the bouncing ball example in Fig. 1, which is not possible in some of the previous work [16] despite its simplicity. Furthermore, an HA learned by our algorithm may involve ODEs with polynomial flow functions, whereas existing work like [20, 21, 26] can infer only HAs with linear ODEs.

Fig. 2 shows the overview of our HA learning algorithm. Our algorithm consists of a *location identification step* and a *transition identification step*. We explain each step below.

Location identification step. To identify the locations, our algorithm first splits trajectories into segments so that each segment consists only of continuous dynamics. To this end, the algorithm estimates the derivative of each point on a trajectory with the *linear multistep method (LMM)* [12] and detects the points where the derivative changes discontinuously.

Then, the segments are grouped into clusters so that the segments in each cluster have similar continuous dynamics. For this, we conduct clustering based on the distance determined by *dynamic time warping (DTW)* [4], which takes two segments and computes their similarity in terms of the “shape.” We treat each cluster as a location of an HA in the following steps.

After the clustering, our algorithm synthesizes an ODE that best describes the continuous dynamics of the segments in each cluster. Our ODE inference is by a template-based approach. For each location, we fix a polynomial template—a polynomial whose coefficients are symbols for unknowns—for the flow function of the ODE. Then, we obtain coefficients of the polynomial via linear regression of the values in a trajectory and the derivative estimated by LMM.

Transition identification step. Once locations are identified, our algorithm next synthesizes the transition relation. It first identifies the pairs of locations (or clusters) between which there is a transition. Concretely, the algorithm identifies a transition from location c_1 to location c_2 if (1) there is a segment s_1 in c_1 and s_2 in c_2 and (2) s_1 immediately precedes s_2 in a trajectory.

The algorithm then synthesizes the guard and the reset on each transition. We synthesize the guard and the reset on each transition in a data-driven manner. Moreover, we introduce type annotation to improve the inference of resets utilizing domain knowledge; we explain the method in detail in Section 3.2.

Contributions Our contributions are summarized as follows.

- We propose an algorithm inferring a general subclass of HAs from a set of input and output trajectories.
- We introduce type annotations to improve the inference of the resets.
- We experimentally show that our algorithm infers HAs fairly close to the original system under learning.

Related Work Despite the maturity of switched-system identification [9, 12], only a few algorithms have been proposed to infer HAs. This scarcity of work in HA learning may be attributed to the additional information that needs to be inferred for HAs (e.g., variable assignments.)

Table 1 summarizes algorithms inferring an HA from a set of trajectories. In [20, 21], an HA is learned from a set of trajectories; however, it does not support systems with inputs. Moreover, only linear ODEs can be learned. In [26],

an HA with inputs and outputs is learned from trajectories, but the learned ODEs are still limited to linear functions. In [16], an HA with polynomial ODEs is learned from inputs and outputs trajectories. However, the guards in the transitions consist only of the input variables and timing constraints. Due to this limitation, their method cannot infer an endogenous HA such as the bouncing ball model in Fig. 1. Compared with these methods, our algorithm supports the most general class of HAs, to our knowledge.

We remark that most of the technical ingredients used in our algorithm are already presented in the previous papers. For example, using LMM for segmentation and inference of polynomial ODEs is also used by Jin et al. [12] for learning switched dynamical systems and we adapted it for learning HA. The use of DTW for clustering is common in [16]. We argue that our significant technical contribution is the achievement of learning the general class of HAs by an appropriate adaptation and combination of these techniques, e.g., by projecting the output dimensions during segmentation. The use of type annotation to improve the inference of variable assignments is also our novelty, up to our knowledge.

Organization After reviewing the preliminaries in Section 2, we present our HA learning algorithm and an experimental evaluation of it in Section 3 and Section 4, respectively. Finally, we conclude in Section 5.

2 Preliminaries

For a set X , we denote its powerset by $\mathcal{P}(X)$. For a pair $p := (a, b)$, we write $pr_1(p)$ for a and $pr_2(p)$ for b . We denote naturals and reals by \mathcal{N} and \mathcal{R} , respectively. For vectors u , and v with the same dimension, the *relative difference* between them is $rd(u, v) := \frac{\|u-v\|}{\|u\|+\|v\|}$ where $\|u\|$ is the Euclidean norm of u . We write $[a, b]$ for the inclusive interval between a and b .

2.1 Trajectories and Hybrid automata

For a time domain $[0, T] \subseteq \mathcal{R}$ and $n \in \mathcal{N}$, an *n-dimensional (continuous) signal* σ is a function assigning an n -dimensional vector $\sigma(t) \in \mathcal{R}^n$ to each timepoint $t \in [0, T]$. Execution of a system with n_1 dimensional inputs and n_2 dimensional outputs can be modeled by an $(n_1 + n_2)$ -dimensional signal.

A *(discrete) trajectory* is a sequence of vectors with timestamps. Concretely, an *n-dimensional trajectory* $(t_1, x_1), (t_2, x_2), \dots, (t_N, x_N)$ is a finite sequence of pairs of timestamp $t_i \in \mathcal{R}$ and the corresponding value $x_i \in \mathcal{R}^n$ satisfying $t_1 < t_2 < \dots < t_N$. For a signal $\sigma: [0, T] \rightarrow \mathcal{R}^n$, a trajectory $(t_1, x_1), (t_2, x_2), \dots, (t_N, x_N)$ is a *discretization* of σ if for any $i \in \{1, 2, \dots, N\}$, we have $x_i = \sigma(t_i)$. We call each vector (t_i, x_i) in a trajectory as a *(sampling) point*.

Hybrid automata (HAs) [3, 14] is a formalism to model a system exhibiting an interplay between continuous and discrete dynamics. Since we aim to learn an HA from a set of trajectories with inputs and outputs, we employ HAs with input and output variables. To define HAs, we fix a finite set of *(continuous state)*

variables \mathcal{X} , input variables \mathcal{I} , and output variables \mathcal{O} such that $\mathcal{X} = \mathcal{I} \uplus \mathcal{O}$. A valuation is a mapping $\delta \in \mathcal{R}^{\mathcal{X}}$ that represents the value of each variable.

Definition 1 (Hybrid automaton). A hybrid automaton (HA) \mathcal{H} , is a tuple $(\mathcal{L}, \text{Inv}, \text{Init}, \text{Flow}, \text{Trans})$ where:

- \mathcal{L} is a finite set of locations;
- $\text{Inv} : \mathcal{L} \rightarrow \mathcal{P}(\mathcal{R}^{\mathcal{X}})$ is a function mapping each location ℓ to the invariant at ℓ ;
- Init , the initial condition, is a pair (ℓ_0, δ_0) such that $\ell_0 \in \mathcal{L}$ and $\delta_0 \in \text{Inv}(\ell_0)$;
- Flow is a flow function mapping each location $\ell \in \mathcal{L}$ to ODEs of the form $\dot{x} = f(x, u)$, called flow equation, where x is the vector of all the variables in \mathcal{O} and u is the vector of all the variables in \mathcal{I} ;
- Trans is the set of discrete transitions denoted by a tuple $e = (\ell, \mathcal{G}, \mathcal{M}, \ell')$, where $\ell, \ell' \in \mathcal{L}$ are the source and target locations, $\mathcal{G} \subseteq \mathcal{P}(\mathcal{R}^{\mathcal{X}})$ is the guard, and $\mathcal{M} : \mathcal{R}^{\mathcal{X}} \rightarrow \mathcal{R}^{\mathcal{O}}$ is the assignment function.

For a transition $e \in \text{Trans}$, we write $\mathcal{G}(e)$ and $\mathcal{M}(e)$ for the guard and the assignment function of e , respectively.

Intuitively, a guard $\mathcal{G}(e)$ of a transition e is the condition that enables the transition: A transition e can be fired if a valuation δ for the variables satisfies $\delta \in \mathcal{G}(e)$. An assignment $\mathcal{M}(e)$ specifies how a valuation is updated if the transition e is fired: A valuation is updated from δ to δ' such that for each $x \in \mathcal{O}$ and $u \in \mathcal{I}$, we have $\delta'(x) = \mathcal{M}(e)(\delta)(x)$ and $\delta'(u) = \delta(u)$ if e is fired.

The semantics of an HA is formalized by the notion of a run. A state of an HA \mathcal{H} is a pair (ℓ, δ) , where ℓ is a location of \mathcal{H} and $\delta \in \mathcal{R}^{\mathcal{X}}$ is a valuation.

Definition 2 (Run). A run of an HA $(\mathcal{L}, \text{Inv}, \text{Init}, \text{Flow}, \text{Trans})$ is a sequence

$$(\ell_0, \delta_0) \xrightarrow{\tau_0} (\ell_0, \delta'_0) \xrightarrow{e_0} (\ell_1, \delta_1) \xrightarrow{\tau_1} (\ell_1, \delta'_1) \xrightarrow{e_1} \dots \xrightarrow{e_{N-1}} (\ell_N, \delta_N) \xrightarrow{\tau_N} (\ell_N, \delta'_N)$$

satisfying $(\ell_0, \delta_0) \in \text{Init}$ and for each $i \in \{0, 1, \dots, N\}$, there are signals $\sigma_i^x : [0, \tau_i] \rightarrow \mathcal{R}^{\mathcal{O}}$ and $\sigma_i^u : [0, \tau_i] \rightarrow \mathcal{R}^{\mathcal{I}}$ such that (i) for any $x \in \mathcal{O}$ and $u \in \mathcal{I}$, we have $\sigma_i^x(0)(x) = \delta_i(x)$ and $\sigma_i^u(0)(u) = \delta_i(u)$, $\sigma_i^x(\tau_i)(x) = \delta'_i(x)$, and $\sigma_i^x(\tau_i)(u) = \delta'_i(u)$, (ii) for any $t \in [0, \tau_i]$, we have $(\sigma_i^x(t), \sigma_i^u(t)) \in \text{Inv}(\ell_i)$ and $\dot{\sigma}_i^x(t) = \text{Flow}(\ell_i)(\sigma_i^x(t), \sigma_i^u(t))$, and (iii) we have $\delta'_i \in \mathcal{G}(e_i)$ and δ_{i+1} is such that for each $x \in \mathcal{O}$ and $u \in \mathcal{I}$, we have $\delta_{i+1}(x) = \mathcal{M}(e_i)(\delta'_i)(x)$ and $\delta_{i+1}(u) = \delta'_i(u)$. For such a run ρ , a signal $\sigma : [0, T_N] \rightarrow \mathcal{R}^{\mathcal{X}}$ is the signal over ρ if σ is such that $\sigma(t)(x) = \sigma_i^x(t - T_{i-1})$ and $\sigma(t)(u) = \sigma_i^u(t - T_{i-1})(u)$ for each $x \in \mathcal{O}$, $u \in \mathcal{I}$, and $i \in \{0, 1, \dots, N\}$ such that $T_i \leq t < T_{i+1}$, where $T_i = \sum_{j=0}^i \tau_j$ and $T_{N+1} = \infty$.

2.2 Linear Multistep Method

The linear multistep method (LMM) [6] is a technique to numerically solve an initial value problem of an ODE $\dot{x}(t) = f(x, t)$. Concretely, it approximates the value of $x(t_{n+M})$ by using the values of $x(t_n), \dots, x(t_{n+M-1})$ and

$f(x_n, t_n), \dots, f(x_{n+M-1}, t_{n+M-1})$ —namely, M previous discretized values of x and $f(x, t)$ —where $t_{n+i} = t_n + ih$ for some $h > 0$. For this purpose, LMM assumes the following approximation parameterized over $(\alpha_i)_i$ and $(\beta_i)_i$:

$$\sum_{i=0}^M \alpha_i x(t_{n-i}) \approx h \sum_{i=0}^M \beta_i f(x(t_{n-i}), t_{n-i}).$$

Then, LMM determines the values of $(\alpha_i)_i$ and $(\beta_i)_i$ so that the error of the above approximation, quantified with Taylor’s theorem, is minimum; see [6, 12, 23] for more detail. The approximation with the determined values of $(\alpha_i)_i$ and $(\beta_i)_i$ is used to successively determine the values of $x(t)$ from its initial value.

In the context of our work, we estimate the derivative of a trajectory at each point without knowing the ODE. To this end, we use *backwards differentiation formula (BDF)* [13, 23] derived from LMM. The idea is to compute the polynomial passing all the points $(t_n, x(t_n)), \dots, (t_{n+M-1}, x(t_{n+M-1}))$ using Lagrange interpolation [6, 13] and derive the formula to approximate the derivative at $(t_{n+M}, x(t_{n+M}))$ from the polynomial using LMM. Concretely, Lagrange interpolation yields the polynomial: $x(t) \approx \sum_{m=0}^M x(t_{n-m}) \prod_{i \neq m} \frac{t - t_{n-i}}{t_{n-m} - t_{n-i}}$. By taking the derivative of both sides and setting t to t_n , we obtain $\dot{x}(t_n) = f(x(t_n), t_n) \approx \sum_{m=0}^M x(t_{n-m}) \prod_{i \neq m} \left(\frac{d}{dt} \frac{t - t_{n-i}}{t_{n-m} - t_{n-i}} \right) \Big|_{t=t_n}$. We use this formula to estimate the derivative at each point in a trajectory. For instance, the formula to estimate the derivatives with $M = 2$ is: $f(x(t_n)) = \frac{1}{h} (\frac{3}{2}x(t_n) - \frac{4}{2}x(t_{n-1}) + \frac{1}{2}x(t_{n-2}))$ [23].

The above formula estimates the derivative at $x(t_n)$ using M previous points—hence called *backward BDF*. Dually, we can derive a formula that estimates the derivative at $x(t_n)$ using M following points called *forward BDF*. We use both in our algorithm.

2.3 Dynamic Time Warping (DTW)

Our algorithm introduced in Section 3 first splits given trajectories so that each segment includes only continuous dynamics. Then, it classifies the generated segments based on the “similarity” of the ODE behind. For the classification purpose, we use *dynamic time warping (DTW)* [4]—one of the methods for quantifying the similarity between time-series data in their shapes—as the measure of the similarity inspired by [16]. The previous work [16] applies DTW for HA learning and confirms its effectiveness.

The DTW distance between two time-series data $X := (x_1, x_2, \dots, x_M)$ and $Y := (y_1, y_2, \dots, y_N)$, where $M, N \in \mathcal{N}$, is defined as follows. The *alignment path* between X and Y is a finite sequence $P := (p_1, \dots, p_l)$ where $p_i \in \{1, 2, \dots, M\} \times \{1, 2, \dots, N\}$ and P is an alignment between $\{1, \dots, M\}$ and $\{1, \dots, N\}$. Concretely, P should satisfy the following conditions: (1) $p_1 = (1, 1)$; (2) $p_l = (M, N)$; (3) $(a_{i+1} - a_i, b_{i+1} - b_i)$ is either $(1, 0)$, $(0, 1)$, or $(1, 1)$ for any $(p_i, p_{i+1}) = ((a_i, b_i), (a_{i+1}, b_{i+1}))$. For example, $((1, 1), (1, 2), (2, 3), (3, 3), (3, 4))$ is an alignment path between (x_1, \dots, x_3) and (y_1, \dots, y_4) .

An alignment path $P = (p_1, \dots, p_l)$ between $X := (x_1, x_2, \dots, x_M)$ and $Y := (y_1, y_2, \dots, y_N)$ determines the sum $d_P := \sum_{i=1}^l \|x_{(pr_1(p_i))} - y_{(pr_2(p_i))}\|$ of the distances between corresponding points in X and Y . Then, the DTW distance $\text{DTW}_{\text{dist}}(X, Y)$ between X and Y is defined by $\min_P d_P$, where P moves all the alignment paths between X and Y . There is an efficient algorithm computing $\text{DTW}_{\text{dist}}(X, Y)$ in $O(MN)$ based on dynamic programming [18].

For X and Y , let P be the alignment that gives the optimal sum of distances between X and Y . We write $\text{DTW}_{\text{correl}}(X, Y)$ for $\text{correl}(P_1, P_2)$, where $P_1 := (pr_1(p_1), \dots, pr_1(p_l))$, $P_2 := (pr_2(p_1), \dots, pr_2(p_l))$, and $\text{correl}(P_1, P_2)$ is the Pearson product-moment correlation coefficients between P_1 and P_2 . This value becomes larger if P_1 and P_2 increase evenly. Thus, the higher this value is, the more X is similar to Y . The effectiveness of this value in classifying segments is also shown in [16].

3 HA Learning from Input–Output Trajectories

Our proposed algorithm is an offline and passive approach for learning automata, which involves observing input-output behavior from a given dataset without interacting with the system during learning. Here, we present our HA learning algorithm from given trajectories. Our problem setting is formalized as follows.

Passive HA learning problem:

INPUT: trajectories $\{(t_1^i, x_1^i), (t_2^i, x_2^i), \dots, (t_{N_i}^i, x_{N_i}^i) \mid i \in \{1, 2, \dots, M\}\}$ that are discretizations of signals over runs of an HA \mathcal{H}

OUTPUT: an HA \mathcal{H} approximating $\bar{\mathcal{H}}$

Our current algorithm learns an HA such that (i) the invariant of each location is **true**, (ii) each guard is expressed as a polynomial inequality, and (iii) each assignment function is a linear function. We assume that (i) each location of \mathcal{H} has different ODEs and (ii) for each pair (ℓ, ℓ') of locations of \mathcal{H} , there is at most one transition from ℓ to ℓ' .

Fig. 2 outlines our HA learning algorithm. We first present the identification of the locations and then present that of the transitions.

3.1 Identification of Locations

We identify the locations of an HA by the following three steps: (i) segmentation of the given trajectories, (ii) clustering of the segments, and (iii) inference of ODEs and initial locations.

Segmentation of the Trajectories The first step in our HA learning algorithm is segmentation. Each trajectory is divided into segments so that the dynamics in each segment are jump-free. We perform segmentation by identifying the change points—the points where the derivative discontinuously changes—along a trajectory. Our approach builds on Jin et al.’s [12] method for learning

Algorithm 1 Outline of our segmentation algorithm

Input: A trajectory $\tau = (t_1, x_1), (t_2, x_2), \dots, (t_N, x_N)$, the step size M in BDF, and the thresholds $\varepsilon_{\text{FwdBwd}}$ and ε_{Bwd}

Output: $cp \subseteq \{1, 2, \dots, N\}$ is the set of change points

```

1:  $candidates \leftarrow \emptyset; C \leftarrow \emptyset$ 
2: for all  $i \in \{M+1, M+2, \dots, N-M\}$  do
3:    $fwd_i \leftarrow f_F(\tau|_{\mathcal{O}}, i, M)$   $\triangleright$  Compute the forward BDF
4:    $bwd_i \leftarrow f_B(\tau|_{\mathcal{O}}, i, M)$   $\triangleright$  Compute the backward BDF
5:   if  $rd(fwd_i, bwd_i) > \varepsilon_{\text{FwdBwd}}$  then
6:     add  $i$  to  $candidates$ 
7: while  $candidates \neq \emptyset$  do
8:    $i \leftarrow \min(candidates)$ ; remove  $i$  from  $candidates$ 
9:   if  $i+1 \notin candidates$  or  $rd(bwd_i, bwd_{i+1}) \geq \varepsilon_{\text{Bwd}}$  then
10:    add  $i$  to  $cp$ 
11:    while  $i+1 \in candidates$  do
12:      remove  $i+1$  from  $candidates$ ;  $i \leftarrow i+1$ 

```

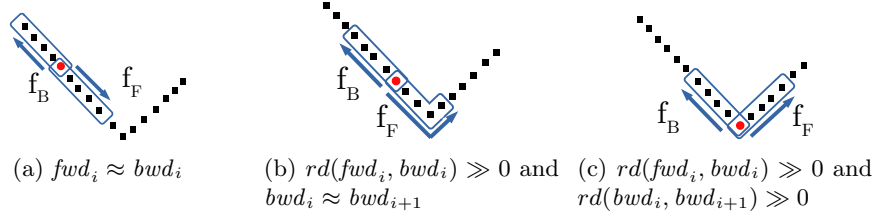


Fig. 3: Illustration of our segmentation algorithm near a boundary of a segment. The red circle in the right figure is the change point because it is the first point satisfying $rd(fwd_i, bwd_i) > \varepsilon_{\text{FwdBwd}}$ and $rd(bwd_i, bwd_{i+1}) > \varepsilon_{\text{Bwd}}$.

switched dynamical systems, but we adapted and modified it to extend the approach for learning hybrid systems.

Algorithm 1 outlines our segmentation algorithm. For simplicity, we present an algorithm for a single trajectory; this algorithm is applied to each trajectory obtained from the system. First, for each point in the trajectory, we estimate the derivative using forward and backward BDF (fwd_i and bwd_i , respectively) and deem the point as a candidate of change points if $rd(fwd_i, bwd_i)$ exceeds the threshold. For example, among the three red circles in Fig. 3, we have $fwd_i \approx bwd_i$ for the one in Fig. 3a and $rd(fwd_i, bwd_i) \gg 0$ for the others. Thus, the red circles in Figs. 3b and 3c are the candidates of the change point. We remark that fwd_i and bwd_i are computed with the trajectory $\tau|_{\mathcal{O}}$ projected to the output variables, and our segmentation is not sensitive to the change in the input variables \mathcal{I} .

When there are consecutive candidates of the change points, we take the first one satisfying $rd(bwd_i, bwd_{i+1}) \geq \varepsilon_{\text{Bwd}}$ to precisely estimate the change point. Such an optimization is justified under the assumption that there are at least $2M - 1$ points between two consecutive mode changes. For example, in the

Algorithm 2 Outline of the clustering of the segmented trajectories

Input: Set Sg of segments and thresholds ε_{dst} and ε_{cor} for distance and diagonality
Output: $C = \{C_1, C_2, \dots, C_n\}$ is a set of set of segments such that each C_i is a cluster

```

1:  $C' \leftarrow \emptyset$ 
2: while  $Sg \neq \emptyset$  do
3:   pick  $sg$  from  $Sg$   $\triangleright$  We still have  $sg \in Sg$  after picking it.
4:    $C' \leftarrow \{sg' \in Sg \mid \text{DTW}_{\text{dist}}(sg|_{\mathcal{O}}, sg'|_{\mathcal{O}}) < \varepsilon_{\text{dst}} \wedge \text{DTW}_{\text{correl}}(sg|_{\mathcal{O}}, sg'|_{\mathcal{O}}) > \varepsilon_{\text{cor}}\}$ 
5:    $Sg \leftarrow Sg \setminus C'$   $\triangleright C'$  always includes  $sg$ , and  $sg$  is removed from  $Sg$ .
6:   add  $C'$  to  $C$ 

```

example shown in Fig. 3, the red circle in Fig. 3c is deemed to be the change point because this is the first candidate satisfying $rd(bwd_i, bwd_{i+1}) \geq \varepsilon_{\text{Bwd}}$. Note that, in inferring ODEs, we consider only the points within a segment that satisfy $rd(fwd_i, bwd_i) \leq \varepsilon_{\text{FwdBwd}}$. This means that candidate points near the boundary of change points are excluded if they do not meet this condition. This is similar to the approach proposed by Jin et al. [12]

The algorithm splits the trajectories at the identified change points into segments; the change points are not included in the segments. Our approach improves upon Jin et al. [12] by adapting their approach for learning switched dynamical systems to the problem of learning hybrid systems. Specifically, we identify change points in a twofold manner. While their approach considers all candidates as change points and drops them from resulting segments, we go a step further and determine the closest change point that precisely separates modes. To achieve this, we search for candidate points until the condition $bwd_i \approx bwd_{i+1}$ is no longer satisfied. This adaptation enables us to include candidate points in the segment actively involved in the transition action, leading to more accurate identification of the transition process.

Clustering of the Segments Then, we cluster the segmented trajectories so that the segments with similar continuous behaviors are included in the same cluster. For instance, in Fig. 2, the continuous behaviors in S_{1a} , S_{2a} , S_{2d} , and S_{3a} are similar and hence included in a single cluster. We use the identified clusters as the set of locations in the resulting HA. This construction is justified when each location has a different ODE.

Algorithm 2 outlines our clustering algorithm. The overall idea is, the algorithm picks one segment (line 3) and creates a cluster by merging similar segments (line 4). We use both DTW_{dist} and $\text{DTW}_{\text{correl}}$ to determine the similarity between segments. We remark that we compare the segments $sg|_{\mathcal{O}}$ and $sg'|_{\mathcal{O}}$ projected to the output variables to ignore the similarity in the input variables.

Inference of ODEs and Initial Locations Our ODE inference is by a template-based linear regression. First, we fix a template $\Phi(x; \theta) = \theta_1 f_1(x) + \theta_2 f_2(x) + \dots + \theta_N f_N(x)$ of the ODE. In our current implementation, each f_i is a monomial whose degree is less than a value specified by a user, but an arbitrary

template can be used. Then, for each cluster C_i and for each output variable $o \in \mathcal{O}$, we construct the set $P_{i,o}$ of points in C_i ,¹ and the derivative of o at this point. Formally, $P_{i,o} = \{(x, \dot{x}(o)) \mid \exists sg \in C_i. x \in sg\}$. The derivative $\dot{x}(o)$ is, for example, computed by BDF. Moreover, we can reuse the derivative used in Algorithm 1. Finally, we use linear regression to compute the coefficients θ such that for each $(x, \dot{x}(o)) \in P_{i,o}$, we have $\dot{x}(o) \approx \Phi(x; \theta)$.

In the resulting HA, the initial locations are the locations such that the corresponding cluster contains the first segment for some trajectories. Therefore, we have multiple initial locations if there are trajectories such that their first segments do not satisfy the similarity condition during clustering.

3.2 Identification of Transitions

After identifying the locations of the resulting HA by clustering the segments, we construct transitions. Let sg_1, sg_2, \dots, sg_m be the segments obtained from a single trajectory by Algorithm 1 and ordered in chronological order; segment sg_i immediately precedes sg_{i+1} in the original trajectory. For each segment sg_g , we denote its initial point, the second last point, and the last point by $sg_g^{\eta_1}$, $sg_g^{\eta_2}$, and $sg_g^{\eta_3}$, respectively.

The idea of the transition identification is to make one transition for each triple $(sg_g^{\eta_2}, sg_g^{\eta_3}, sg_{g+1}^{\eta_1})$ —called a *connection triple*—and use these points in a triple to infer its guard and assignment; see Fig. 4 for an illustration. We note that such a triple is always defined since each segment has at least three points.

Formally, for clusters C_i and C_j and a segmented trajectory sg_1, sg_2, \dots, sg_m , the set $T_{i,j}$ of connection triples from C_i to C_j is as follows:

$$T_{i,j} = \{(sg_g^{\eta_2}, sg_g^{\eta_3}, sg_{g+1}^{\eta_1}) \mid g \in \{1, 2, \dots, m-1\}, sg_g \in C_i, sg_{g+1} \in C_j\}$$

If there are multiple trajectories in HA learning, we construct $T_{i,j}$ for each trajectory and take their union.

We infer guards and assignments using $T_{i,j}$. For each cluster pair (C_i, C_j) , the guard of the transition from C_i to C_j is obtained using a support vector machine (SVM) to classify the second last points and the last points. More precisely, for $T_{i,j}^\perp = \{sg_g^{\eta_2} \mid \exists (sg_g^{\eta_2}, sg_g^{\eta_3}, sg_{g+1}^{\eta_1}) \in T_{i,j}\}$ and $T_{i,j}^\top = \{sg_g^{\eta_3} \mid \exists (sg_g^{\eta_2}, sg_g^{\eta_3}, sg_{g+1}^{\eta_1}) \in T_{i,j}\}$, we compute an equation of hyperplane separating $T_{i,j}^\perp$ and $T_{i,j}^\top$ using SVM and construct an inequality constraint \mathcal{G} that is satisfied by the points in $T_{i,j}^\top$ but not by that in $T_{i,j}^\perp$.

For each cluster pair (C_i, C_j) , the assignment in the transition from C_i to C_j is obtained using linear regression to approximate the relationship between the valuation before and after the transition. More precisely, we use linear regression

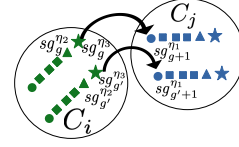


Fig. 4: Illustration of the points connecting clusters C_i and C_j

¹ Notice that, as mentioned above, we only consider the points within a segment that satisfy $rd(fwd_i, bwd_i) \leq \varepsilon_{\text{FwdBwd}}$.

to compute an equation \mathcal{M} such that for each $(sg_g^{\eta_2}, sg_g^{\eta_3}, sg_{g+1}^{\eta_1}) \in T_{i,j}$ and for each $x \in \mathcal{O}$, $sg_{g+1}^{\eta_1}(x)$ is close to $\mathcal{M}(sg_g^{\eta_3})(x)$. Such \mathcal{M} is used as the assignment.

Improving Assignments Inference with Type Annotation If we have no prior knowledge of the system under learning, we infer assignments using linear regression, as mentioned above. However, even if the exact system dynamics are unknown, we often know how each variable behaves at jumps. For instance, it is reasonable to believe that a variable representing temperature is continuous; hence, it does not change its value at jumps. Such domain knowledge is helpful in inferring precise assignments rather than one using linear regression.

To easily enforce the constraints from domain knowledge on variables, we extend our assignment inference to allow users to annotate each variable with types expressing how a variable is assumed to behave at jumps. We currently support the following types.

No assignments If a variable is continuous at a jump (e.g., the variable representing temperature mentioned above), one annotates the variable with “no assignments”. For a variable x with this annotation, the procedure above infers an assignment that does not change the value of x .

Constant assignments If the value assigned to a variable at a jump is a fixed constant, we annotate the variable with “constant assignments”. For instance, in the bouncing ball HA depicted in Fig. 1, the variable x is reset to 0 upon reaching the ground or when the guard condition is satisfied.

Constant pool If the value assigned to a variable at a jump is chosen from a finite set, one annotates the variable with “Constant pool” accompanied with the finite set $\{v_1, \dots, v_n\}$. An example of such a variable is one representing the gear in a model of an automotive. For a variable with this annotation, our algorithm infers the assignment at a jump by majority poll: For a transition from cluster C_i to C_j , it chooses the value most frequently occurring in $T_{i,j}$ as $sg_{g+1}^{\eta_1}$.

3.3 Impact of Parameter Selection on Model Accuracy

We recognize the complexity and potential challenges inherent in ensuring that our proposed hybrid automaton closely emulates the original black-box system, given the intricate and often nonlinear dynamics at play. Nevertheless, our methodology is developed to capture the crucial behaviors of the original system, serving as a foundation for further analysis and understanding. In our method, specific tuning parameters play pivotal roles during the segmentation and clustering processes. To illustrate, the parameter $\varepsilon_{\text{FwdBwd}}$ contributes significantly to effective segmentation, while ε_{Bwd} facilitates pinpointing the correct transition point, which in turn allows for the accurate inference of data points for guards and assignments. It is critical to mention that the choice of these thresholds must be well-thought-out. For instance, a large value for $\varepsilon_{\text{FwdBwd}}$ might

overlook some change points, while a smaller value could lead to unnecessary redundancy. Therefore, depending on the dynamical class of the system under study, these thresholds may require careful adjustments.

Similarly, during the clustering process, the thresholds DTW_{dist} and $\text{DTW}_{\text{correl}}$ play instrumental roles in establishing efficient similarity comparisons between segments. While a $\text{DTW}_{\text{correl}}$ of 0.8 typically works well in deciding segment similarity, the co-adjustment of DTW_{dist} and $\text{DTW}_{\text{correl}}$ parameters effectively allows the clustering process to manage the number of modes in the learned hybrid automaton, balancing precision in the process. In essence, the judicious selection of these parameters is integral to the success of our method in learning an accurate hybrid automaton.

In addition, it is crucial to emphasize that the accuracy of the learned hybrid automaton heavily depends on the amount of data available. We have adapted our segmentation process and ODE inference from the approach presented by Jin et al. [12], which provides bounds for estimation errors based on sampling time step and a priori knowledge of system dynamics. While perfect replication of the black-box system may not be achievable, the goal is to construct a meaningful and practical model within the framework of a hybrid automaton. See Table 1 for a comparison of these methods.

4 Experiments

We implemented our proposed algorithm using a combination of C++, Python, and MATLAB/Simulink/Stateflow: The HA learning algorithm is written in Python; The learned model is translated into a Simulink/Stateflow model by a C++ program; We use MATLAB to simulate the learned model. We optimized the ODE inference by using only a part of the trajectories when they were sufficiently many. We take $M = 5$ as the step size for BDF. Our implementation is available at <https://github.com/rajgurung777/HybridLearner> and the artifact at <https://doi.org/10.5281/zenodo.7934743>.

We conducted experiments (i) to compare the performance of our algorithm against a state-of-the-art method and (ii) to evaluate how the type annotation helps our learning algorithm. For the former evaluation, we compared our algorithm against one of the latest HA learning methods called POSEHAD [16]. Among the recent hybrid-automata learning methodologies, POSEHAD is the closest to ours in that (1) it handles hybrid systems with nonlinear ODEs and (2) it supports input signals to a system; see Table 1. We compared our algorithm with and without a type annotation for the latter evaluation, denoted as “Type” and “W/o Type,” respectively. We also compared our method with two other methods (HAutLearn [26] and HySynthParametric [21]); the result is presented in Section 4.3.

In the upcoming comparisons in Sections 4.2 and 4.3, our proposed method is contrasted with several existing approaches, including POSEHAD, HAutLearn, and HySynthParametric. While noteworthy in their respective areas, these methods have certain limitations when it comes to handling the comprehensive fea-

tures of hybrid automata - a challenge our method is designed to overcome. Specifically, our approach manages all crucial aspects of hybrid automata, such as guards, nonlinear ODEs, assignments, and support for input signals. It’s important to underline that the purpose of these comparisons is not to downplay these existing methods but to highlight the unique scope of functionality and adaptability our method brings to exploring hybrid automata. While this may give an initial impression of an unbalanced comparison, it’s essential to emphasize the comprehensive capabilities of our approach, designed to address the gaps left by these other notable methods.

Each benchmark consists of a Simulink/Stateflow model, which we call an *original model*, and two sets of trajectories generated from the original model, which we call *training* and *test* sets. We generated trajectories by feeding random input trajectories and random initial values of the state variables to the original model. The training set is used to learn an HA, which we call a *learned model*, and the test set is used to evaluate the accuracy of the learned model. For each benchmark, the size of the training and test sets are 64 and 32, respectively.

To evaluate the accuracy of the learned model, we feed the same input trajectories and the same initial values to the original and the learned models and compared their output trajectories. The comparison is based on the DTW distance DTW_{dist} . A low DTW distance indicates higher accuracy of the learned model. We denote as δ_{O_1} and δ_{O_2} the DTW distances between trajectories generated from the original and the learned model on the output variable, O_1 , and O_2 , respectively. We note that, in POSEHAD, the DTW distance is not computed with the entire trajectories but with the segmented trajectories. All the experiments reported in this paper are conducted on a machine with an Intel Core i9 CPU, 2.40GHz, and 32 GiB RAM. We used $\varepsilon_{\text{Bwd}} = 0.01$ in all our experiments.

4.1 Benchmark Description

We briefly describe the benchmarks used in our experiments.

BALL This is a benchmark modeling a bouncing ball taken from the demo example of Simulink [2]. Fig. 1 shows the HA. The acceleration due to the gravity g is taken as input. The range of g is $[-9.9, -9.5]$. We modify the original Simulink model to parameterize the initial values of x and v . We also set the model to operate on a fixed-step solver. We let $x \in [10.2, 10.5]$ and $v = 15$. The reset factor c in Fig. 1 is $c = -0.8$. We execute the model for a time horizon of 13 units with a sampling time of 0.001, i.e., each trajectory consists of 13,000 points. We use $\varepsilon_{\text{FwdBwd}} = 0.1$, $\varepsilon_{\text{dst}} = 9.0$, and $\varepsilon_{\text{cor}} = 0.8$.

TANKS This benchmark models a two tanks system [11]. Fig. 7a shows the HA. The system consists of two tanks with liquid levels x_1 and x_2 . The first tank has in/out flow controlled by a valve v_1 , whereas, the second tank has outflow controlled by the other valve v_2 . Both tanks have external in/out flow controlled by the input signal u . There is also a flow from the first tank to the second tank.

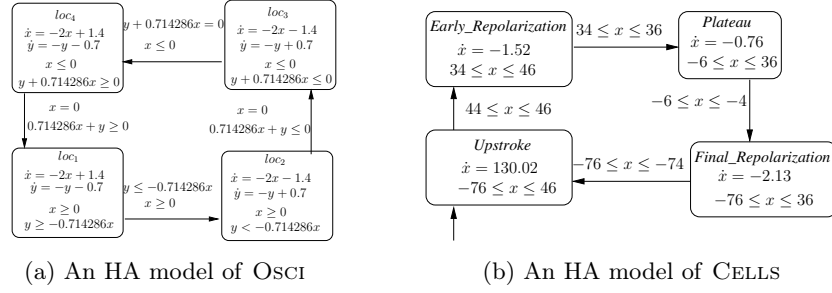


Fig. 5: HA models for OSCI and CELLS benchmarks

In summary, the system has four locations for on and off of v_1 and v_2 . The range of the input is $u \in [-0.1, 0.1]$, the initial liquid level of the two tanks are $x_1 = 1.2$ and $x_2 = 1$, and the initial location is *off_off*. We execute the model for a time horizon of 9.3 units with a sampling time of 0.001, i.e., each trajectory consists of 9,300 points. We use $\varepsilon_{\text{FwdBwd}} = 0.01$, $\varepsilon_{\text{dst}} = 1.5$ and $\varepsilon_{\text{cor}} = 0.7$.

OSCI This is a benchmark modeling a switched oscillator without filters [8]. OSCI is an affine system with two variables, x and y oscillating between two equilibria to maintain a stable oscillation. The HA is shown in Fig. 5a. All the transitions have constant assignments. This system has no inputs. The initial values are $x, y \in [0.01, 0.09]$, and the initial location is *loc1*. We execute the model for a time horizon of 10 units with a sampling time of 0.01, i.e., each trajectory consists of 1,000 points. We use $\varepsilon_{\text{FwdBwd}} = 0.1$, $\varepsilon_{\text{dst}} = 1.0$ and $\varepsilon_{\text{cor}} = 0.89$.

CELLS This is a benchmark modeling excitable cells [10, 27], which is a biological system exhibiting hybrid behavior. We use a variant of the excitable cell used in [22]. Our HA model is shown in Fig. 5b. This model has no inputs. We take the initial values for the voltage $x \in [-76, -74]$. The *Upstroke* is the initial location. We execute the model for a time horizon of 500 units with a sampling time of 0.01, i.e., each trajectory consists of 50,000 points. We use $\varepsilon_{\text{FwdBwd}} = 0.01$, $\varepsilon_{\text{dst}} = 1.0$, and $\varepsilon_{\text{cor}} = 0.92$.

ENGINE This benchmark models an engine timing system taken from the demo examples in the Simulink automotive category [1]. The model is a complex non-linear system with two inputs and one output signal. The inputs are the desired speed of the system and the load torque, while the output signal is the engine's speed. We simulate the model for a time horizon of 10 units with a sampling time of 0.01, i.e., each trajectory consists of 1,000 points. We use $\varepsilon_{\text{FwdBwd}} = 0.99$, $\varepsilon_{\text{dst}} = 560$ and $\varepsilon_{\text{cor}} = 0.89$.

4.2 Results and Discussion

Table 2: Summary of the results. The columns δ_{O_1} and δ_{O_2} show the minimum (Min), maximum(Max), average (Avg), and standard deviation (Std) of the DTW distance between trajectories generated by the original model and the learned model feeding the test set. The columns Time show the total running time in seconds for learning an HA. Cells with the best results are highlighted.

Model	Measure	W/o Type			Type			POSEHAD		
		δ_{O_1}	δ_{O_2}	Time	δ_{O_1}	δ_{O_2}	Time	δ_{O_1}	δ_{O_2}	Time
BALL	Min(δ)	0.15	0.27	351.2	0.15	0.27	336.7	127.0	1.5e+6	41535.9
	Max(δ)	16.4	12.1		16.4	12.1		39660.7	8.3e+8	
	Avg(δ)	1.8	2.1		1.8	2.1		9566.2	1.7e+8	
	Std(δ)	3.3	3.1		3.3	3.1		12695.3	1.8e+8	
TANKS	Min(δ)	0.1	0.3	383.1	0.003	0.005	383.5	37.8	7.8e+12	13771.5
	Max(δ)	3.9	2.6		3.2	2.6		2.3e+4	2.0e+14	
	Avg(δ)	0.9	1.3		0.2	0.3		8.1e+3	9.5e+13	
	Std(δ)	1.0	0.68		0.8	0.74		7.6e+3	5.9e+13	
OSCI	Min(δ)	0.21	0.3	24.1	0.17	0.2	24.9	15.8	8.8	404.2
	Max(δ)	0.4	0.7		0.3	0.6		1.5e+3	933.9	
	Avg(δ)	0.3	0.3		0.2	0.2		1.2e+3	716.0	
	Std(δ)	0.04	0.1		0.03	0.09		404.0	313.4	
CELLS	Min(δ)	13.2	–	2404.2	1.3	–	2358.5	2.5e+9	–	191050.0
	Max(δ)	155.3	–		150.5	–		5.1e+9	–	
	Avg(δ)	63.9	–		58.1	–		3.1e+9	–	
	Std(δ)	53.9	–		57.3	–		8.3e+8	–	
ENGINE	Min(δ)	2.2e+4	–	50.6	3.2e+4	–	47.9	2.8e+3	–	197.6
	Max(δ)	1.7e+5	–		5.4e+4	–		4.2e+14	–	
	Avg(δ)	6.6e+4	–		4.2e+4	–		1.3e+13	–	
	Std(δ)	4.8e+4	–		5.5e+3	–		7.4e+13	–	

Overall Discussion Table 2 shows the summary of the results. In columns δ_{O_1} and δ_{O_2} , we observe that for all the benchmarks, the HAs learned by our algorithm (both “W/o Type” and “Type”) achieved higher accuracy in terms of Avg(δ). This is because of the adequate handling of the input variables and the inference of the resets at transitions. Moreover, type annotation improves model accuracy, as shown in benchmarks TANKS, OSCI, CELLS, and ENGINE. However, in BALL, both methods perform equally.

We also observe that for the HAs learned by our learning algorithm, the maximum DTW distance Max(δ) tends to be close to the minimum DTW distance Min(δ). This indicates that trajectories generated by our learned model do not have a high deviation from the trajectories generated by the original model. We discuss the detail later in this section. In contrast, in the POSEHAD algorithm, they tend to have a high difference between Min(δ) and Max(δ). We also observe that for the HAs learned by the POSEHAD algorithm, the standard deviation Std(δ) is much larger than that learned from ours. This suggests that our learning algorithm is better at generalization. Moreover, our algorithm takes much

less time than POSEHAD. For instance, in the CELLS benchmark, our algorithm takes less than one hour, whereas POSEHAD takes more than 53 hours.

Discussion for each benchmark Fig. 6 shows the learned HA for BALL produced by our algorithm with a type annotation. We observe that the ODE is precisely learned. Although the guard is far from the expected condition $x \leq 0$, it is close to the expected condition given the range of the state variables; for instance when we have $v \approx -20.55$ and $g \approx -9.8$, the condition is about $x \leq 0.020$, which is reasonably close to $x \leq 0$. Furthermore, our algorithm accurately inferred the assignment of v as $v ::= -0.8v$. In Figs. 8a and 8b, we show plots of the trajectories obtained from the HAs learned by our algorithm (with and without type annotation), the output trajectory predicted by POSEHAD, and the trajectory obtained from the original model. In Fig. 8b, we did not include the predicted trajectory by POSEHAD due to its high error. We observe that the trajectories obtained from our learned models coincide with the original benchmark trajectory, while the trajectory predicted by POSEHAD does not.

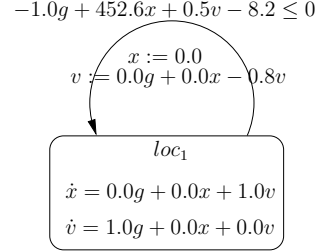


Fig. 6: The HA learned by our algorithm with type annotation on BALL

Fig. 7b shows the HA learned by our algorithm with type annotation on the TANKS benchmark. Since the initial value, $x_2 = 1$, is satisfied by the guard at the initial location, the system takes an instant transition to location *off_on* (see Fig. 7a). Therefore, all trajectories contain data starting from this location, and our algorithm identifies this to be the initial location. Moreover, the trajectories given to the learning algorithm do not include data visiting the location *on_on*, and this mode is not present in the learned model. We observe that the ODEs are exactly learned, and the guards are close to the original model. In Fig. 8c, we show a plot of the trajectories obtained from the HAs learned by our algorithm (with and without type annotation), the output trajectory predicted by

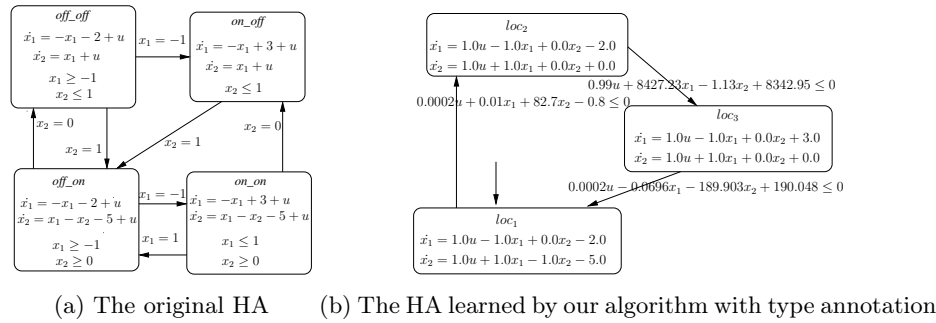


Fig. 7: HAs on TANKS benchmark

POSEHAD, and the trajectory obtained from the original model. The models learned by our algorithm produced trajectories close to the original model, while several parts predicted by POSEHAD are far from the original one.

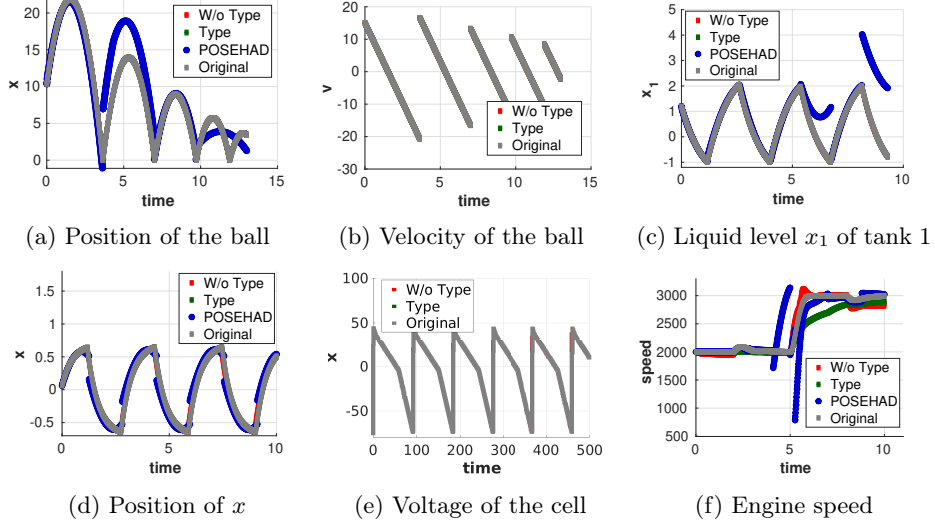


Fig. 8: Trajectories on (a-b) BALL (c) TANKS (d) OSCI (e) CELLS and (f) ENGINE

For the ENGINE model, due to the system’s complexity, our algorithm produced HAs at most with 37 locations and 137 transitions. In Fig. 8f, we show a plot of the trajectories obtained from the HAs learned by our algorithm (with and without type annotation), the output trajectory predicted by POSEHAD, and the trajectory obtained from the original model. The models learned by our algorithm produced trajectories uniformly close to the original model, while several parts predicted by POSEHAD are far from the original one. Similar observations on accuracy can be drawn from Figs. 8d and 8e on OSCI and CELLS benchmarks, respectively.

4.3 Comparison with other methods

We compared our proposed approach with other state-of-the-art methods: HAuLearn [26] and HySynthParametric [21]. We conducted this experiment using only OSCI, which does not take an input signal, since HAuLearn and HySynthParametric do not support a model taking inputs; see Table 1.

The result is shown in Fig. 9. Figs. 9a and 9b (resp., Figs. 9c and 9d) show the plots obtained by the learned models trained with five (resp., 64) trajectories. The training time with five trajectories was as follows: 60.9 seconds for HAuLearn; 15.6 seconds for HySynthParametric; 2.2 seconds for ours. The training time with 64 trajectories was as follows: 1442.3 seconds for HAuLearn; 1483.6 seconds for HySynthParametric; 24.9 seconds for ours.

For the experiment with five training trajectories, the HA learned by HAuLearn is as precise as our method. However, for the experiment with 64 training

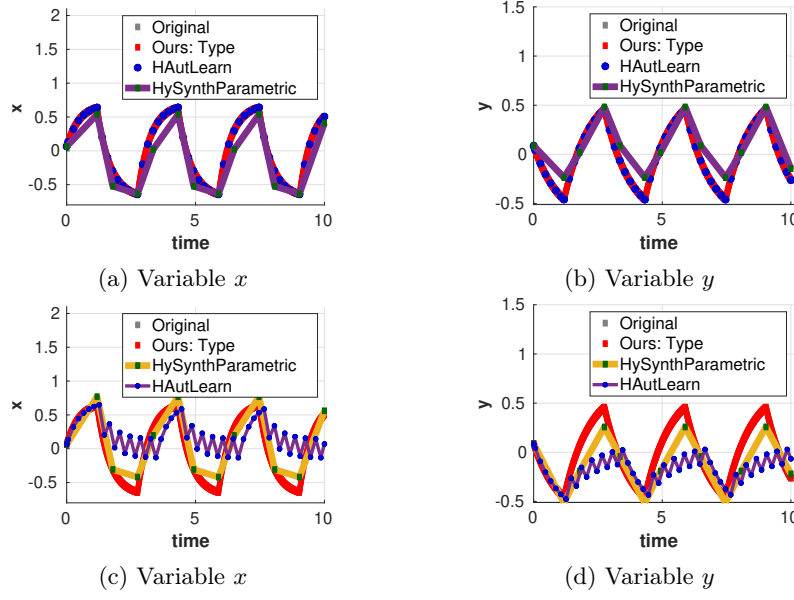


Fig. 9: Trajectories obtained from the learned HAs on the OSCI benchmark by the three tools. (a) and (b) are trained using five trajectories, while (c) and (d) show models trained using 64 trajectories.

trajectories, we observed that the switching guard in the HA learned by HAutLearn allowed the model to take an early jump from the second jump onwards, thus generating plots that do not coincide with the original trajectories. We can observe that the HA learned by HySynthParametric is less precise than ours.

The performance of HAutLearn was largely affected by the values of multiple parameters. The plots in Fig. 9 is obtained by tuning parameters through trials and errors.

5 Conclusion

This paper presents an algorithm to learn an HA with polynomial ODEs from input-output trajectories. We identify the locations by segmenting the given trajectories, clustering the segments, and inferring ODEs. We learn transition guards using SVM with a polynomial kernel and assignment functions using linear regression. Our experimental evaluation suggests that our algorithm produces more accurate HAs than the state-of-the-art algorithms. Moreover, we extended the inference of assignments with type annotations to utilize prior knowledge of a user. In future work, we plan to utilize our learned HA model to perform black-box checking [15, 19, 24] for falsification, model-bounded monitoring of hybrid systems [25], and controller synthesis [7, 17].

Acknowledgements We are grateful to the anonymous reviewers for their valuable comments. This work was partially supported by JST CREST Grant No. JPMJCR2012, JST PRESTO Grant No. JPMJPR22CA, JST ACT-X Grant No. JPMJAX200U, and JSPS KAKENHI Grant No. 22K17873 & 19H04084.

Bibliography

- [1] MathWorks: Engine Timing Model with Closed Loop Control. <https://in.mathworks.com/help/simulink/slref/engine-timing-model-with-closed-loop-control.html>, accessed: 2022-12-29
- [2] MathWorks: Simulation of Bouncing Ball. <https://in.mathworks.com/help/simulink/slref/simulation-of-a-bouncing-ball.html>, accessed: 2022-12-29
- [3] Alur, R., Courcoubetis, C., Halbwachs, N., Henzinger, T.A., Ho, P.H., Nicollin, X., Olivero, A., Sifakis, J., Yovine, S.: The algorithmic analysis of hybrid systems. *Theoretical Computer Science* **138**(1), 3–34 (1995)
- [4] Bellman, R., Kalaba, R.: On adaptive control processes. *IRE Transactions on Automatic Control* **4**(2), 1–9 (1959)
- [5] Bortolussi, L., Policriti, A.: Hybrid systems and biology. In: Bernardo, M., Degano, P., Zavattaro, G. (eds.) *Formal Methods for Computational Systems Biology*, 8th International School on Formal Methods for the Design of Computer, Communication, and Software Systems, SFM 2008, Bertinoro, Italy, June 2–7, 2008, Advanced Lectures. *Lecture Notes in Computer Science*, vol. 5016, pp. 424–448. Springer (2008). https://doi.org/10.1007/978-3-540-68894-5_12, https://doi.org/10.1007/978-3-540-68894-5_12
- [6] Butcher, J.C.: *Numerical methods for ordinary differential equations*. John Wiley & Sons (2016)
- [7] Filippidis, I., Dathathri, S., Livingston, S.C., Ozay, N., Murray, R.M.: Control design for hybrid systems with tulip: The temporal logic planning toolbox. 2016 IEEE Conference on Control Applications (CCA) (Sep 2016). <https://doi.org/10.1109/cca.2016.7587949>, <http://dx.doi.org/10.1109/CCA.2016.7587949>
- [8] Frehse, G., Le Guernic, C., Donzé, A., Cotton, S., Ray, R., Lebeltel, O., Ripado, R., Girard, A., Dang, T., Maler, O.: SpaceEx: Scalable Verification of Hybrid Systems. In: Ganesh Gopalakrishnan, S.Q. (ed.) *Proc. 23rd International Conference on Computer Aided Verification (CAV)*. pp. 379–395. LNCS, Springer (2011), <http://spaceex.imag.fr>
- [9] Garulli, A., Paoletti, S., Vicino, A.: A survey on switched and piecewise affine system identification. *IFAC Proceedings Volumes* **45**(16), 344–355 (Jul 2012). <https://doi.org/10.3182/20120711-3-be-2027.00332>, <http://dx.doi.org/10.3182/20120711-3-be-2027.00332>
- [10] Grosu, R., Mitra, S., Ye, P., Entcheva, E., Ramakrishnan, I.V., Smolka, S.A.: Learning cycle-linear hybrid automata for excitable cells. In: Bemporad,

- A., Bicchi, A., Buttazzo, G.C. (eds.) Hybrid Systems: Computation and Control, 10th International Workshop, HSCC 2007, Pisa, Italy, April 3-5, 2007, Proceedings. Lecture Notes in Computer Science, vol. 4416, pp. 245–258. Springer (2007). https://doi.org/10.1007/978-3-540-71493-4_21, https://doi.org/10.1007/978-3-540-71493-4_21
- [11] Hiskens, I.A.: Stability of limit cycles in hybrid systems. In: Proceedings of the 34th Annual Hawaii International Conference on System Sciences. pp. 6–pp. IEEE (2001)
 - [12] Jin, X., An, J., Zhan, B., Zhan, N., Zhang, M.: Inferring switched nonlinear dynamical systems. *Formal Aspects of Computing* **33**(3), 385–406 (2021)
 - [13] Keller, R.T., Du, Q.: Discovery of dynamics using linear multistep methods. *SIAM Journal on Numerical Analysis* **59**(1), 429–455 (2021)
 - [14] Lygeros, J., Tomlin, C., Sastry, S.: Hybrid systems: modeling, analysis and control. Electronic Research Laboratory, University of California, Berkeley, CA, Tech. Rep. UCB/ERL M **99**, 6 (2008)
 - [15] Peled, D.A., Vardi, M.Y., Yannakakis, M.: Black box checking. In: Wu, J., Chanson, S.T., Gao, Q. (eds.) *Formal Methods for Protocol Engineering and Distributed Systems, FORTE XII / PSTV XIX'99, IFIP TC6 WG6.1 Joint International Conference on Formal Description Techniques for Distributed Systems and Communication Protocols (FORTE XII) and Protocol Specification, Testing and Verification (PSTV XIX)*, October 5-8, 1999, Beijing, China. IFIP Conference Proceedings, vol. 156, pp. 225–240. Kluwer (1999)
 - [16] Saberi, I., Faghieh, F., Bavil, F.S.: A passive online technique for learning hybrid automata from input/output traces. *ACM Trans. Embed. Comput. Syst.* **22**(1) (oct 2022). <https://doi.org/10.1145/3556543>, <https://doi.org/10.1145/3556543>
 - [17] Saoud, A., Jagtap, P., Zamani, M., Girard, A.: Compositional abstraction-based synthesis for cascade discrete-time control systems. In: Abate, A., Girard, A., Heemels, M. (eds.) *6th IFAC Conference on Analysis and Design of Hybrid Systems, ADHS 2018, Oxford, UK, July 11-13, 2018. IFAC-PapersOnLine*, vol. 51, pp. 13–18. Elsevier (2018). <https://doi.org/10.1016/j.ifacol.2018.08.003>, <https://doi.org/10.1016/j.ifacol.2018.08.003>
 - [18] Senin, P.: Dynamic time warping algorithm review. *Information and Computer Science Department University of Hawaii at Manoa Honolulu, USA* **855**(1-23), 40 (2008)
 - [19] Shijubo, J., Waga, M., Suenaga, K.: Efficient black-box checking via model checking with strengthened specifications. In: Feng, L., Fishman, D. (eds.) *Runtime Verification - 21st International Conference, RV 2021, Virtual Event, October 11-14, 2021, Proceedings. Lecture Notes in Computer Science*, vol. 12974, pp. 100–120. Springer (2021). https://doi.org/10.1007/978-3-030-88494-9_6, https://doi.org/10.1007/978-3-030-88494-9_6
 - [20] Soto, M.G., Henzinger, T.A., Schilling, C.: Synthesis of hybrid automata with affine dynamics from time-series data. In: Bogomolov, S., Jungers, R.M. (eds.) *HSCC '21: 24th ACM International Conference on Hybrid Sys-*

- tems: Computation and Control, Nashville, Tennessee, May 19–21, 2021. pp. 2:1–2:11. ACM (2021). <https://doi.org/10.1145/3447928.3456704>, <https://doi.org/10.1145/3447928.3456704>
- [21] Soto, M.G., Henzinger, T.A., Schilling, C.: Synthesis of parametric hybrid automata from time series. In: Bouajjani, A., Holík, L., Wu, Z. (eds.) Automated Technology for Verification and Analysis - 20th International Symposium, ATVA 2022, Virtual Event, October 25–28, 2022, Proceedings. Lecture Notes in Computer Science, vol. 13505, pp. 337–353. Springer (2022). https://doi.org/10.1007/978-3-031-19992-9_22, https://doi.org/10.1007/978-3-031-19992-9_22
 - [22] Soto, M.G., Henzinger, T.A., Schilling, C., Zeleznik, L.: Membership-based synthesis of linear hybrid automata. In: Dillig, I., Tasiran, S. (eds.) Computer Aided Verification - 31st International Conference, CAV 2019, New York City, NY, USA, July 15–18, 2019, Proceedings, Part I. Lecture Notes in Computer Science, vol. 11561, pp. 297–314. Springer (2019). https://doi.org/10.1007/978-3-030-25540-4_16, https://doi.org/10.1007/978-3-030-25540-4_16
 - [23] Süli, E., Mayers, D.F.: An introduction to numerical analysis. Cambridge university press (2003)
 - [24] Waga, M.: Falsification of cyber-physical systems with robustness-guided black-box checking. In: Ames, A.D., Seshia, S.A., Deshmukh, J. (eds.) HSCC '20: 23rd ACM International Conference on Hybrid Systems: Computation and Control, Sydney, New South Wales, Australia, April 21–24, 2020. pp. 11:1–11:13. ACM (2020). <https://doi.org/10.1145/3365365.3382193>, <https://doi.org/10.1145/3365365.3382193>
 - [25] Waga, M., André, E., Hasuo, I.: Model-bounded monitoring of hybrid systems. ACM Trans. Cyber-Phys. Syst. **6**(4) (nov 2022). <https://doi.org/10.1145/3529095>, <https://doi.org/10.1145/3529095>
 - [26] Yang, X., Beg, O.A., Kenigsberg, M., Johnson, T.T.: A framework for identification and validation of affine hybrid automata from input-output traces. ACM Trans. Cyber Phys. Syst. **6**(2), 13:1–13:24 (2022). <https://doi.org/10.1145/3470455>, <https://doi.org/10.1145/3470455>
 - [27] Ye, P., Entcheva, E., Grosu, R., Smolka, S.A.: Efficient modeling of excitable cells using hybrid automata. In: Proc. of CMSB. vol. 5, pp. 216–227 (2005)

A Additional Detailed

A.1 Experiment settings

For our experiment in Table 2, the maximum number of trajectory segments we take for each location in the ODE inference helps our algorithm improve performance compared to POSEHAD. For the benchmarks BALL, TANKS, and OSCI, we take 50 trajectory segments, 100 for ENGINE, and 3 for CELLS, respectively.

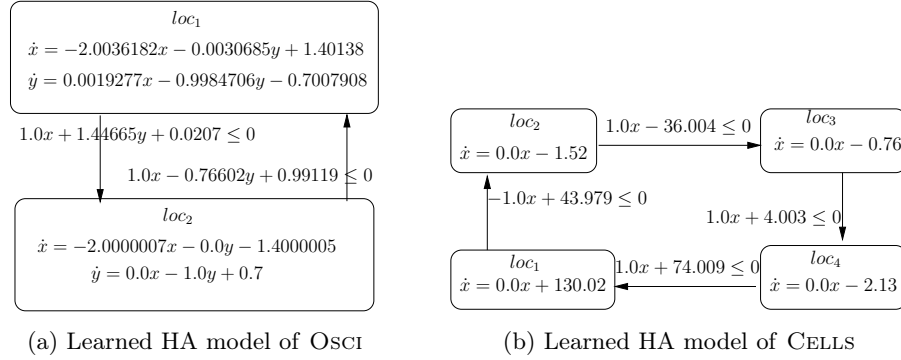


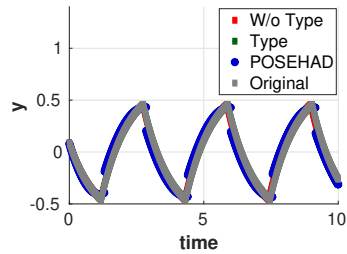
Fig. 10: Our learned HA models using type annotation

We thank the authors for providing us with the source code of the POSEHAD algorithm. POSEHAD also uses the DTW algorithm for clustering similar segmented trajectories. However, for segmentation, they use a different off-the-shelf Python library named Rupture to detect change points in trajectories. Therefore, the threshold parameters that we use for our algorithm may not be the best for POSEHAD. So, as recommended in their paper, we perform a simple manual grid search of parameters, including the thresholds used in our approach. We fix a parameter that performs the best and keeps the implementation running without returning errors during the entire search. In the original POSEHAD implementation, pre-processing is applied to the input-output data by scaling the data values to 0 and 1. To perform a fair comparison, we skip this pre-processing in the experiment. POSEHAD learns an HA model for each output variable independently.

A.2 Additional experimental results

Detailed discussion for each benchmark

Fig. 10a shows our learned HA model for an OSCI model generated using the Type annotation approach. Observe that in the original model, locations loc_1 and loc_4 have the same ODE, and there is no assignment logic (cause for a change point) for a discrete transition. Therefore our segmentation process considers these locations to be a single mode. Similarly, locations loc_2 and loc_3 have the same dynamics, so our approach also learns a single location for this. The ODE and the transition guards in the learned model are relatively close to the original model. In Figs. 8d and 11, we compare output trajectories obtained by our learned models (with and without Type annotation), POSEHAD prediction, and the original benchmark.

Fig. 11: Trajectories of OSCI model on variable y

The trajectory obtained by our learned model using Type annotation overlaps precisely with the original benchmark trajectory. Without a Type annotation, the trajectory either overlaps or passes close to the original trajectory. On the other hand, several sections of the predicted trajectory by POSEHAD are either incorrectly predicted or do not overlap with the original trajectory.

[Fig. 10b](#) shows our learned HA model for the CELLS model produced using the Type annotation approach. We learned a four-location HA with deterministic guards for each transition. Note that the learned ODE is exact to the original model for the associated locations, and the guard conditions are close to the actual guards. In [Fig. 8e](#), we show the accuracy of our learned model where trajectories generated by our learned models (with and without Type annotation) coincide with the trajectory obtained by the original benchmark. Due to high errors, we could not show the predicted trajectory by POSEHAD here in a single figure.